ACS Catalysis

Research Article

pubs.acs.org/acscatalysis

Solar-Driven Z-scheme Water Splitting Using Modified $BaZrO_3$–$BaTaO_2N$ Solid Solutions as Photocatalysts

Kazuhiko Maeda,*[†,‡] Daling Lu,[§] and Kazunari Domen*[∥]

[†]Department of Chemistry, Graduate School of Science and Engineering, Tokyo Institute of Technology, 2-12-1-NE-2 Ookayama, Meguro-ku, Tokyo 152-8550, Japan

[‡]Precursory Research for Embryonic Science and Technology (PRESTO), Japan Science and Technology Agency (JST), 4-1-8 Honcho Kawaguchi, Saitama 332-0012, Japan

[§]Center for Advanced Materials Analysis, Tokyo Institute of Technology, 2-12-1 Ookayama, Meguro-ku, Tokyo 152-8550, Japan

[∥]Department of Chemical System Engineering, The University of Tokyo, 7-3-1 Hongo, Bunkyo-ku, Tokyo 113-8656, Japan

Supporting Information

ABSTRACT: A two-step photocatalytic water splitting (Z-scheme) system consisting of a modified $BaZrO_3$–$BaTaO_2N$ solid solution, a paired photocatalyst, and a reversible donor/acceptor pair (i.e., redox mediator) was constructed. $BaZrO_3$–$BaTaO_2N$ (Zr/Ta = 0.05) having a band gap of 1.8 eV has sufficient potential to reduce and oxidize water by absorbing visible photons of up to 660 nm. Upon suitable modification of this material with nanoparticulate cocatalysts, both H_2 and O_2 were evolved individually in the presence of reversible redox couples (viz., IO_3^-/I^- and Fe^{3+}/Fe^{2+}), although O_2 evolution from aqueous solution containing Fe^{3+} was negligible. Among various combinations tested, $BaZrO_3$–$BaTaO_2N$ modified with Pt nanoparticles was the most suitable for H_2 evolution in the presence of an IO_3^-/I^- pair, achieving Z-scheme water splitting into H_2 and O_2 in combination with either PtO_x/WO_3 or TiO_2 rutile as an O_2 evolution photocatalyst even under simulated sunlight.

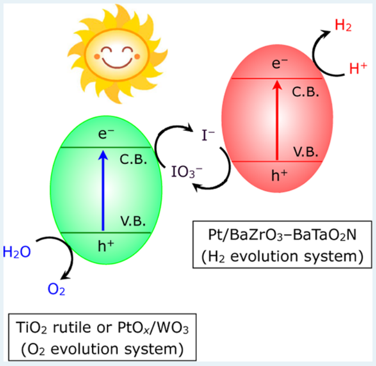

KEYWORDS: *cocatalyst, heterogeneous photocatalysis, hydrogen production, oxynitride, solar energy conversion, water splitting, Z-scheme*

1. INTRODUCTION

Water splitting on a particulate photocatalyst is one of the most suitable choices toward large-scale solar to hydrogen energy conversion.[1] Recently, photocatalytic water splitting driven by a two-step photoexcitation using two different semiconductor photocatalysts, which is the so-called Z-scheme water splitting, has been studied as a means of producing H_2 from water utilizing a wide range of visible light.[2] Since Bard introduced the concept of Z-scheme water splitting in 1979,[3] many efforts have been made to construct such systems, with a focus on the development of both new materials and effective electron relays.[3−17] From the viewpoint of solar energy conversion, it is important to develop a Z-scheme system that exhibits high quantum yield at a given wavelength and operates under a wide range of the solar spectrum.[1] While several Z-scheme water-splitting systems have been developed, a satisfactory system has not been devised so far.

Our group has studied (oxy)nitrides as potential photocatalysts for Z-scheme water splitting. The most advantageous aspect of (oxy)nitrides for application in the Z-scheme is that they are capable of harvesting a wide range of visible photons, depending on the compositions. Among (oxy)nitrides examined, $BaTaO_2N$ has the longest absorption edge that can harvest up to 660 nm photons, working as a H_2 evolution photocatalyst in the presence of an IO_3^-/I^- shuttle redox mediator.[11] Very recently, activation of $BaTaO_2N$ to improve photocatalytic activity for H_2 evolution from water was achieved by forming a solid solution with $BaZrO_3$.[16] The improvement is attributable to the increased driving force for the redox reactions and the reduced density of defects, which minimizes the undesirable electron−hole recombination. It has also proven that a $BaZrO_3$–$BaTaO_2N$ (Zr/Ta $\leq$ 0.1) solid solution having a single phase perovskite structure is capable of reducing and oxidizing water even under >660 nm irradiation.[18] However, water reduction and oxidation using $BaZrO_3$–$BaTaO_2N$ in the presence of reversible electron donor/acceptor pairs for application in Z-scheme water splitting have yet to be investigated in detail.

This paper reports a more systematic study on $BaZrO_3$–$BaTaO_2N$ solid solution as a photocatalyst not only for H_2 evolution but also for O_2 evolution in Z-scheme water splitting. Solar-driven Z-scheme water splitting is also demonstrated for the first time using an oxynitride material as a building block for Z-scheme water splitting.

Received: February 27, 2013
Revised: March 30, 2013
Published: April 5, 2013

dx.doi.org/10.1021/cs400156m | *ACS Catal.* 2013, 3, 1026−1033

2. EXPERIMENTAL SECTION

2.1. Materials and Reagents. A $BaZrO_3$−$BaTaO_2N$ solid solution (Zr/Ta = 0.05 by mole) was prepared according to a method reported previously.[18] WO_3 (High Purity Chemicals, 99.99%), TiO_2 Rutile (Aldrich, 99.99%), TaON, and $BiVO_4$ were employed as O_2 evolution photocatalysts for two-step water splitting. TaON, ZrO_2/TaON (Zr/Ta = 0.1), and $BiVO_4$ were prepared according to previous methods.[13,19] Figure 1 shows UV−visible diffuse reflectance spectra of these samples.

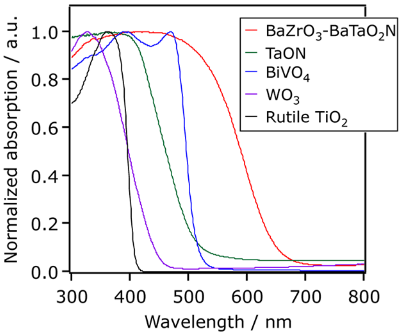

Figure 1. Diffuse reflectance spectra of the particulate photocatalysts used in this study.

$RuCl_3 \cdot nH_2O$ (Kanto Chemicals, 99.9%), $RhCl_3 \cdot xH_2O$ (Aldrich, 38−40% Rh), $(NH_4)_2PdCl_4$ (Kanto Chemicals, 37% Pd), $Na_2IrCl_6 \cdot 6H_2O$ (Kanto Chemicals, 97% Ir), $H_2PtCl_6 \cdot 2H_2O$ (Kanto Chemicals, 97% Pt), and $HAuCl_4 \cdot 4H_2O$ (Kanto Chemicals, 99.0%) were used as cocatalyst precursors for $BaZrO_3$−$BaTaO_2N$ and some O_2 evolution photocatalysts. NaI (Kanto Chemicals, reagent grade), $NaIO_3$ (Kanto Chemicals, reagent grade), $FeCl_2 \cdot 4H_2O$ (Wako Pure Chemicals, 99.0−102.0%), and $FeCl_3 \cdot 6H_2O$ (Wako Pure Chemicals, 99.0%) were employed as redox reagents. All chemicals were used without further purification.

2.2. Modification with Cocatalysts. Modification of $BaZrO_3$−$BaTaO_2N$ with nanoparticulate metal cocatalysts was accomplished by impregnation to improve the water reduction activity. A 0.2−0.3 g portion of $BaZrO_3$−$BaTaO_2N$ powder was immersed in an aqueous solution (2−3 mL) containing various amounts of metal precursor in a water bath. After drying the solution, the resulting powder was collected, and heated in H_2 gas flow (20 mL·min^{-1}) at 473 K for 1 h.

For IrO_2 loading, a colloidal IrO_2 solution was first prepared by hydrolysis of Na_2IrCl_6 according to the previous method with some modification.[20] Briefly, 0.016 g of Na_2IrCl_6 was dissolved in 50 mL of H_2O, and the pH of the solution was adjusted to 11−12 with aqueous NaOH solution. The solution was heated at 353 K for 0.5 h, and then cooled to room temperature by immersion in an ice−water bath. The pH of the cooled solution was then adjusted slowly to 9 with aqueous HNO_3 solution. Subsequent heating at 353 K for 0.5 h resulted in a deep blue solution containing colloidal IrO_2, which was diluted to 50 mL in total volume. A 0.12−0.13 g portion of a sample was then dispersed in the as-prepared colloidal IrO_2 solution of about 30 mL (1.5 wt % with respect to catalyst mass), with some dilution. The suspension was subject to agitation for 1 h at room temperature, followed by centrifugation to collect residual solids. UV−visible spectroscopy showed that in all cases, there was no absorption signal derived from IrO_2 colloids in the supernatant solution thus-obtained, indicating that quantitative adsorption of IrO_2 was achieved in the present IrO_2 concentration range examined. The IrO_2-loaded samples were then dried in an oven at 343 K overnight.

For WO_3 and TaON, PtO_x and RuO_2 were respectively loaded as reaction promoters for O_2 evolution, as in previous reports.[7d,12,17] PtO_x (0.5 wt % as Pt)-loaded WO_3 was prepared by immersing WO_3 in aqueous H_2PtCl_6 solution, followed by calcination in air at 823 K for 0.5 h. RuO_2 (0.5 wt %)-loaded TaON was prepared in a similar manner, using $RuCl_3$ as the precursor, followed by calcination in air at 573 K for 1 h.

2.3. Characterization of Catalysts. The prepared samples were studied by powder X-ray diffraction (XRD; RINT-UltimaIII, Rigaku; Cu Kα), UV−visible diffuse reflectance spectroscopy (DRS; V-560, JASCO), X-ray photoelectron spectroscopy (XPS; JPS-9000, JEOL), and high-resolution transmission electron microscopy (HR-TEM; JEM-2010F, Jeol). The binding energies determined by XPS were corrected by reference to the C 1s peak (284.6 eV) for each sample. The Brunauer−Emmett−Teller (BET) surface area was measured using a BELSORP-mini instrument (BEL Japan) at liquid nitrogen temperature (77 K).

2.4. Photocatalytic Reactions. Reactions were carried out in a Pyrex top-irradiation reaction vessel connected to a glass closed gas circulation system. Unless otherwise stated, metal-loaded $BaZrO_3$−$BaTaO_2N$ as an H_2 evolution photocatalyst (50 mg) and an O_2 evolution photocatalyst (100 mg) were suspended using a magnetic stirrer in aqueous solutions (100 mL) containing different concentrations of a redox mediator. The pH of the solutions was controlled by adding aqueous H_2SO_4 or NaOH if necessary. For individual H_2 and O_2 evolution, $BaZrO_3$−$BaTaO_2N$ modified with a cocatalyst (50 mg) was dispersed in aqueous solution (100 mL) containing electron donors (I^- or Fe^{2+}) of acceptors (IO_3^- or Fe^{3+}) in a similar manner but without pH adjustment. The reactant solutions were evacuated several times to completely remove any air prior to irradiation under a 300 W xenon lamp. The irradiation wavelength was controlled by a combination of a cold mirror (CM-1) and a water filter ($350 < \lambda < 800$ nm). For visible light irradiation, a cutoff filter (L42) was fitted to the above-mentioned light source ($420 < \lambda < 800$ nm). The spectral feature of this light source can be found elsewhere.[21] The reactant solution was maintained at room temperature by a water bath during the reaction. The evolved gases were analyzed by gas chromatography (Shimadzu, GC-8A with TCD detector and MS-5A column, argon carrier gas). The reproducibility of the gas evolution rate was typically within 10−15% under a given set of reaction conditions.

Solar energy conversion efficiency (η) was calculated according to the following equation:

$$\eta(\%) = R_H \cdot \Delta G^0/(P \cdot S) \times 100 \tag{1}$$

where R_H, ΔG^0, P, and S indicate the rate of hydrogen evolution (mol·s^{-1}) in Z-scheme water splitting, standard Gibbs energy of water (237.13×10^3 J·mol^{-1}), the intensity of simulated sunlight (100 mW·cm^{-2}) from a solar simulator (Asahi Spectra, HAL-320) and irradiation area (16 cm^2), respectively. The irradiance of the solar simulator almost (ca. 95%) corresponds to that of AM1.5G.

3. RESULTS AND DISCUSSION

3.1. Structural Characterization of $BaZrO_3-BaTaO_2N$.

As the physicochemical character of the as-prepared $BaZrO_3-BaTaO_2N$ solid solution has been reported previously,[18] the results of structural characterization on this material are included in Supporting Information. XRD analysis showed that the as-prepared sample exhibited a single-phase perovskite structure similar to $BaTaO_2N$ (Supporting Information, Figure S1). The DRS spectrum of $BaZrO_3-BaTaO_2N$ indicates that the compound absorbs visible photons up to 660 nm (Figure 1). The particle size of $BaZrO_3-BaTaO_2N$ ranges from 50 to 200 nm with some aggregation, as shown in Supporting Information, Figure S1. The specific surface area determined by nitrogen adsorption at liquid nitrogen temperature (77 K) was about 6.5 $m^2 \cdot g^{-1}$.

3.2. Effect of Modification of $BaZrO_3-BaTaO_2N$ with Metal Cocatalysts on Z-scheme Water Splitting Activity.

First, we examined the effect of modification of $BaZrO_3-BaTaO_2N$ with various metal cocatalysts on Z-scheme water splitting from aqueous NaI solution (1.0 mM) in the presence of PtO_x/WO_3 as an O_2 evolution photocatalyst, because unmodified $BaZrO_3-BaTaO_2N$ did not work as a H_2 evolution photocatalyst. The metals (Ru, Rh, Pd, Ir, Pt, and Au) tested as cocatalysts have been reported to function as a H_2 evolution site on a heterogeneous photocatalyst for water splitting.[22,23] It is also noted that, although both $BaZrO_3-BaTaO_2N$ and WO_3 have absorption bands near 660 and 450 nm, respectively (Figure 1), the reactions were conducted under ultraviolet (UV) and visible irradiation ($350 < \lambda < 800$ nm) to utilize more photons to obtain more products. As listed in Table 1, simultaneous H_2 and O_2 evolution was achieved only when Pt was loaded as a cocatalyst, indicating the occurrence of water splitting reaction. The water-splitting reaction was initiated by photooxidation of I^- into IO_3^- and photoreduction of H^+ into H_2 on $Pt/BaZrO_3-BaTaO_2N$ catalyst, after which photoreduction of IO_3^- into I^- and photooxidation of H_2O into O_2 occurred on PtO_x/WO_3 catalyst as follows.

Table 1. Effect of Modification of $BaZrO_3-BaTaO_2N$ with Various Metal Cocatalysts (0.3 wt %) on Z-scheme Water Splitting Activities in Combination with PtO_x/WO_3 and IO_3^-/I^- Shuttle Redox Mediator[a]

entry	cocatalyst	amount of evolved gases for 3 h/μmol	
		H_2	O_2
1	None	0	0
2	Ru	0	0
3	Rh	0.3	0
4	Pd	0.1	0
5	Ir	0.3	0
6	Pt	67.4	27.9
7	Au	0	0

[a] Reaction conditions: catalyst, 100 mg of PtO_x/WO_3 and 50 mg of metal-loaded $BaZrO_3-BaTaO_2N$; aqueous NaI solution, 100 mL (1.0 mM); light source, xenon lamp (300 W) fitted with a cold mirror (CM-1); reaction vessel, Pyrex top-irradiation type; irradiation wavelength, $350 < \lambda < 800$ nm.

$$I^- + 6h^+ + 6OH^- \rightarrow IO_3^- + 3H_2O \quad \text{(photooxidation of } I^- \text{ into } IO_3^-\text{)} \tag{2}$$

$$2H^+ + 2e^- \rightarrow H_2 \quad \text{(photoreduction of } H^+ \text{ into } H_2\text{)} \tag{3}$$

$$IO_3^- + 6e^- + 3H_2O \rightarrow I^- + 6OH^- \quad \text{(photoreduction of } IO_3^- \text{ into } I^-\text{)} \tag{4}$$

$$4OH^- + 4h^+ \rightarrow O_2 + 2H_2O \quad \text{(photooxidation of } H_2O \text{ into } O_2\text{)} \tag{5}$$

Because Pt was found to be the most effective cocatalyst among those examined (Table 1, entry 6), the effect of Pt-loading amount onto $BaZrO_3-BaTaO_2N$ was investigated. Changing the amount of Pt loaded onto the $BaZrO_3-BaTaO_2N$ had a significant impact on the water splitting rate, as shown in Figure 2. With increasing Pt loading, the rates of H_2 and O_2 evolution both increased abruptly, reaching a maximum at around 0.3–0.5 wt %, then decreasing. In addition, the H_2/O_2 ratio of the products was close to 2 when the loading amount was in the optimal range. The abrupt increase in Z-scheme water splitting activity after Pt-loading on $BaZrO_3-BaTaO_2N$ suggests that the relatively inefficient step for this reaction is the water reduction process.

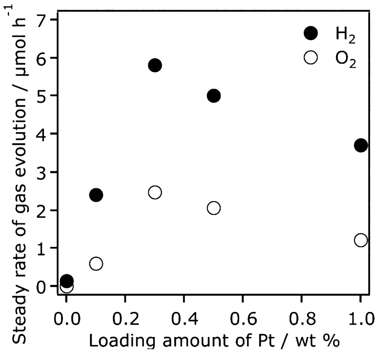

Figure 2. Dependence of the rates of H_2 and O_2 evolution over a mixture of PtO_x/WO_3 and $Pt/BaZrO_3-BaTaO_2N$ on the loading amount of Pt. Reaction conditions: catalyst, 100 mg of PtO_x/WO_3 and 50 mg of $Pt/BaZrO_3-BaTaO_2N$; aqueous NaI solution, 100 mL (1.0 mM); light source, xenon lamp (300 W) fitted with a cold mirror (CM-1) and a cutoff filter (L42); reaction vessel, Pyrex top-irradiation type; irradiation wavelength, $420 < \lambda < 800$ nm.

Thus, the amount of Pt cocatalyst loading was an important factor determining the efficiency of the two-step water splitting system consisting of $Pt/BaZrO_3-BaTaO_2N$ and PtO_x/WO_3 in the presence of an IO_3^-/I^- shuttle redox mediator. The observed trend between water-splitting rate and Pt-loading is very similar to those observed in similar Z-scheme systems using Pt-loaded semiconductors as H_2 evolution photocatalysts.[10b,13b] Increasing the loading amount of Pt results in an increase in the density of active sites for H_2 evolution, while the decrease in activity with higher Pt loading is likely to be associated with aggregation of Pt nanoparticles on $BaZrO_3-BaTaO_2N$, which can reduce the active surface available for H_2 evolution, thereby contributing to a decrease in activity. HR-TEM images of the same samples are shown in Supporting Information, Figure S2. Pt nanoparticles smaller than 2 nm were dispersed in the optimized catalyst.

The electronic state of the loaded Pt species on $BaZrO_3-BaTaO_2N$ was thus investigated by XPS. According to our previous report, Pt species introduced by impregnation followed by H_2 reduction at 473 K are almost entirely metallic, but somewhat electron-deficient.[13b] As shown in Supporting Information, Figure S3, the peak position of $4f_{7/2}$ electrons in the prepared catalyst is slightly higher than that in a Pt foil reference, but not as much as $Pt^{II}O$ species appearing at binding energies of about 73.0−73.5 eV ($4f_{7/2}$ electrons),[24] consistent with our previous report.[13b]

3.4. Effect of O_2 Evolution Photocatalyst and Redox Mediator.

Table 2 lists the activities of Z-scheme water splitting systems under UV and visible irradiation ($350 < \lambda < 800$ nm) in which 0.3 wt % Pt-loaded $BaZrO_3$−$BaTaO_2N$ was used as a building block for H_2 evolution with various O_2 evolution photocatalysts (PtO_x/WO_3, TiO_2 rutile, $RuO_2/TaON$, or $BiVO_4$). When Pt/$BaZrO_3$−$BaTaO_2N$ and NaI were respectively employed as an H_2 evolution photocatalyst and an electron mediator, PtO_x/WO_3 and TiO_2 rutile photocatalysts achieved nearly stoichiometric H_2 and O_2 evolution (entries 1 and 2), indicating the occurrence of water splitting. On the other hand, $BiVO_4$ and $RuO_2/TaON$ did not produce appreciable H_2 and O_2 evolution (entries 3 and 4).

Table 2. Effect of O_2 Evolution Photocatalyst and Redox Mediator on Z-scheme Water Splitting Activities Using 0.3 wt % Pt/$BaZrO_3$−$BaTaO_2N$ as a H_2 Evolution Photocatalyst[a]

			amount of evolved gases for 3 h/μmol	
entry	paired O_2 evolution photocatalyst	reactant solution	H_2	O_2
1	PtO_x/WO_3	NaI 1.0 mM	67.4	27.9
2	TiO_2 rutile	NaI 1.0 mM	63.8	28.4
3	$BiVO_4$	NaI 1.0 mM	tr.	0
4[b]	$RuO_2/TaON$	NaI 0.2 mM	0.4	tr.
5	PtO_x/WO_3	$FeCl_2$ 10 mM	tr.	0
6	$BiVO_4$	$FeCl_2$ 10 mM	0.5	0
7	$BiVO_4$	$FeCl_2$ 5.0 mM	0.3	0
8	$BiVO_4$	$FeCl_2$ 1.0 mM	0.1	0
9[c]	TiO_2 rutile	$FeCl_2$ 10 mM	5.7	tr.

[a] Reaction conditions: catalyst, 50 mg of Pt/$BaZrO_3$−$BaTaO_2N$ and 100 mg of an O_2 evolution photocatalyst; aqueous solution, 100 mL; light source, xenon lamp (300 W) fitted with a cold mirror (CM-1); reaction vessel, Pyrex top-irradiation type; irradiation wavelength, $350 < \lambda < 800$ nm. [b] $RuO_2/TaON$ 50 mg. [c] The time course data is displayed in Supporting Information, Figure S4.

It has been reported that an Fe^{3+}/Fe^{2+} redox couple acts as an effective electron mediator for some two-step water splitting systems consisting of Rh-doped $SrTiO_3$ (H_2 evolution system) and an O_2 evolution photocatalyst such as $BiVO_4$ or WO_3.[9a] Interestingly, however, the combination of Pt/$BaZrO_3$−$BaTaO_2N$ with either PtO_x/WO_3 or $BiVO_4$ did not produce any appreciable H_2 and O_2 from an aqueous solution containing Fe^{2+} as an electron donor (entries 5−8). In contrast, employing TiO_2 rutile resulted in observable H_2 and O_2 evolution, although the rates were relatively slow (entry 9) in the initial 3 h of reaction, compared to an analogous system using an IO_3^-/I^- redox mediator (entry 2). In this case, there was an induction period for O_2 evolution, with a large deviation in the ratio of H_2/O_2 from the stoichiometry, in which Fe^{3+}, the oxidation product by the valence band holes in Pt/$BaZrO_3$−$BaTaO_2N$, was presumably accumulated in the solution up to a certain level. The H_2/O_2 ratio gradually became stoichiometric with reaction time, although it does not exactly meet the stoichiometry (Supporting Information, Figure S4). Simultaneous H_2 and O_2 evolution was not achievable if one component of the system (either Pt/$BaZrO_3$−$BaTaO_2N$, TiO_2 rutile, $FeCl_2$, or light) is absent. These results strongly suggest that Z-scheme water splitting proceeds over a mixture of Pt/$BaZrO_3$−$BaTaO_2N$ and TiO_2 rutile in the presence of an Fe^{3+}/Fe^{2+} redox mediator under irradiation. This is the first example of achieving simultaneous H_2 and O_2 evolution from water containing an Fe^{3+}/Fe^{2+} redox mediator using an oxynitride material. TiO_2 rutile is known to possess unique photocatalytic activity for water oxidation even in the presence of electron-donating species such as Fe^{2+} and I^-,[6b,7d] which would lead to the successful water splitting in combination with Pt/$BaZrO_3$−$BaTaO_2N$ in the presence of an Fe^{3+}/Fe^{2+} redox mediator. The whole scheme can be described as follows:

$$Fe^{2+} + h^+ \rightarrow Fe^{3+} \quad (\text{photooxidation of } Fe^{2+} \text{ into } Fe^{3+}) \tag{6}$$

$$2H^+ + 2e^- \rightarrow H_2 \quad (\text{photoreduction of } H^+ \text{into } H_2) \tag{7}$$

$$Fe^{3+} + e^- \rightarrow Fe^{2+} \quad (\text{photoreduction of } Fe^{3+} \text{ into } Fe^{2+}) \tag{8}$$

$$4OH^- + 4h^+ \rightarrow O_2 + 2H_2O \quad (\text{photooxidation of } H_2O \text{ into } O_2) \tag{9}$$

Thus, the strong effects of the paired O_2 evolution photocatalyst and redox mediator on Z-scheme water splitting using Pt/$BaZrO_3$−$BaTaO_2N$ were highlighted. It was thought that these characteristic behaviors in reactivity with respect to O_2 evolution photocatalysts and redox mediators arise primarily from the different reactivity of Pt/$BaZrO_3$−$BaTaO_2N$ with the redox mediators employed. To examine this possibility, H_2 evolution by Pt/$BaZrO_3$−$BaTaO_2N$ alone in the presence of NaI or $FeCl_2$ as an electron donor was investigated. Figure 3 shows the time courses of H_2 evolution from aqueous NaI and $FeCl_2$ solution (10 mM) using Pt/$BaZrO_3$−$BaTaO_2N$. As reported previously, Pt/$BaZrO_3$−$BaTaO_2N$ photocatalytically produces H_2 from an aqueous solution containing NaI as an electron donor.[16] However, the rate of H_2 evolution decreases as the reaction proceeds. This deactivation is ascribed to the backward reaction (photoreduction of IO_3^- by photogenerated electrons), which takes place in the conduction band of the catalyst.[2b] When I^- is used as an electron donor for H_2 evolution with Pt/$BaZrO_3$−$BaTaO_2N$, IO_3^- is produced by the photooxidation of I^- by valence band holes. As IO_3^- is more susceptible to reduction than H^+ (IO_3^-/I^-, +0.67 V; H^+/H_2, −0.41 V vs NHE at pH 7), H_2 evolution ceases when the concentration of IO_3^- reaches a certain level.[2b] When the reaction was carried out in the presence of both I^- (10 mM) and IO_3^- (1.0 mM), the rate of H_2 evolution decreased markedly, providing evidence for the above competitive model. Similar behavior has been observed for some Pt-loaded photocatalysts such as anatase-TiO_2, $SrTiO_3$:Cr/Ta, TaON, and ZrO_2/TaON in H_2 evolution from aqueous NaI solution.[7,10,11,13b] The H_2 evolution behavior from aqueous $FeCl_2$ solution was similar to the NaI case, indicating Pt/$BaZrO_3$−$BaTaO_2N$ is able to reduce H^+ into H_2 using Fe^{2+} as an electron donor.

It was shown that Pt/$BaZrO_3$−$BaTaO_2N$ has the ability to oxidize both I^- and Fe^{2+}. Nevertheless, it was difficult to achieve simultaneous H_2 and O_2 evolution in the presence of an

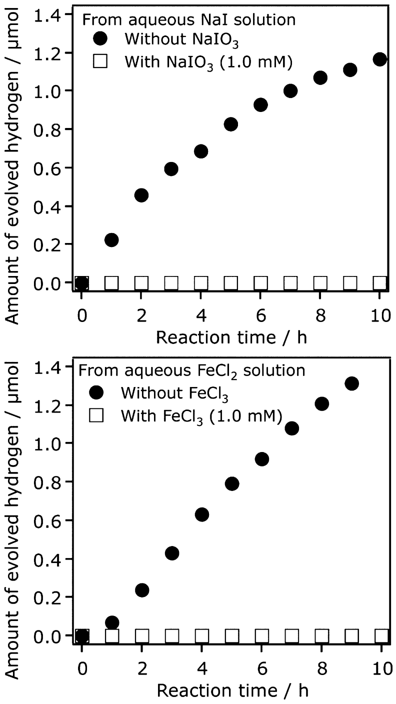

Figure 3. Time courses of H_2 evolution over 0.3 wt % Pt/$BaZrO_3$−$BaTaO_2N$ from NaI and $FeCl_2$ solution. Reaction conditions: catalyst, 50 mg; aqueous solution, 100 mL (10 mM); light source, xenon lamp (300 W) fitted with a cold mirror (CM-1); reaction vessel, Pyrex top-irradiation type; irradiation wavelength, 350 < λ < 800 nm.

Fe^{3+}/Fe^{2+} redox couple (except for the TiO_2 rutile case), as shown in Table 2 (entries 5−9). The reactivity of the valence band holes in Pt/$BaZrO_3$−$BaTaO_2N$ with Fe^{2+} was examined by changing the concentration of Fe^{2+}. Taking the Pt/$BaZrO_3$−$BaTaO_2N$ + $BiVO_4$ system for example, the H_2 evolution rate increased with increasing the concentration of $FeCl_2$ from 1.0 to 10 mM (entries 6−8, Table 2). The increase in $FeCl_2$ concentration leads in turn to the competitive oxidation of Fe^{2+} on O_2 evolution photocatalysts (the backward reaction of eq 8), making it difficult to achieve water oxidation and the resulting stoichiometric H_2 and O_2 evolution. As will be displayed later, on the other hand, increasing the concentration of NaI from 0 to 0.5 mM resulted in a sharp increase in H_2 evolution (also O_2 evolution in this case) to reach a plateau at 0.5−2.0 mM concentration range. These results suggest that the oxidation of Fe^{2+} by holes in the valence band of Pt/$BaZrO_3$−$BaTaO_2N$ is relatively slow, while that of I^- is efficient, even though the oxidation potential of Fe^{2+} (+0.77 V vs NHE at pH = 0) is more negative than that of I^- (+1.08 V vs NHE at pH = 0). The successful conversion of I^- into IO_3^- by Pt/$BaZrO_3$−$BaTaO_2N$ allowed for simultaneous H_2 and O_2 evolution in combination with O_2 evolution photocatalysts that are active for the reduction of IO_3^- into I^- under band gap irradiation.[7] Negligible O_2 evolution was observed from RuO_2/TaON and $BiVO_4$ because water oxidation by these materials is significantly suppressed in the presence of I^-, even at the low levels resulting from the preferential oxidation of I^-.[7d,12] Therefore, Pt/$BaZrO_3$−$BaTaO_2N$ is a useful component for H_2 evolution in the two-step water splitting with an IO_3^-/I^- redox mediator.

3.5. Effect of NaI Concentration and pH. The effect of reaction conditions was further investigated using Pt/$BaZrO_3$−$BaTaO_2N$ in combination with either PtO_x/WO_3 or TiO_2 rutile, which were relatively active combinations (entries 1 and 2, Table 2). Figure 4 shows the time course of H_2 and O_2 evolution for a mixture of 0.3 wt % Pt/$BaZrO_3$−$BaTaO_2N$ and PtO_x/WO_3 from 1.0 mM aqueous NaI solution under visible light (420 < λ < 800 nm). There was an induction period at the beginning of the reaction, after which the rates of H_2 and O_2 evolution became almost constant. As discussed above, the induction period may be due to the accumulation of IO_3^- in the solution up to a certain level.[7d] The steady rates of H_2 and O_2 evolution recorded at different NaI concentrations are plotted in Figure 5. No gas evolution was observed in the absence of NaI. With increasing NaI concentration, the rates of H_2 and O_2 evolution both improved significantly, reaching a maximum at around 1−2 mM with nearly stoichiometric H_2/O_2 ratio. However, further increase in NaI concentration to 5.0 mM resulted in activity-drop.

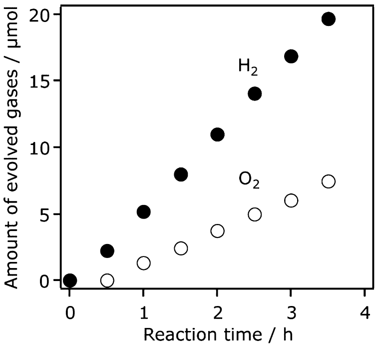

Figure 4. Time course of H_2 and O_2 evolution over a mixture of 0.3 wt % Pt/$BaZrO_3$−$BaTaO_2N$ and PtO_x/WO_3. Reaction conditions: catalyst, 100 mg of PtO_x/WO_3 and 50 mg of Pt/$BaZrO_3$−$BaTaO_2N$; aqueous NaI solution, 100 mL (1.0 mM); light source, xenon lamp (300 W) fitted with a cold mirror (CM-1) and a cutoff filter (L42); reaction vessel, Pyrex top-irradiation type; irradiation wavelength, 420 < λ < 800 nm.

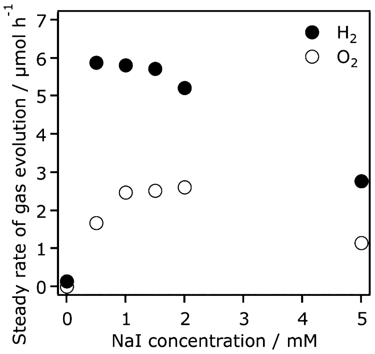

Figure 5. Dependence of the rates of H_2 and O_2 evolution over a mixture of PtO_x/WO_3 and 0.3 wt % Pt/$BaZrO_3$−$BaTaO_2N$ on the concentration of NaI. Reaction conditions: catalyst, 100 mg of PtO_x/WO_3 and 50 mg of Pt/$BaZrO_3$−$BaTaO_2N$; aqueous NaI solution, 100 mL; light source, xenon lamp (300 W) fitted with a cold mirror (CM-1) and a cutoff filter (L42); reaction vessel, Pyrex top-irradiation type; irradiation wavelength, 420 < λ < 800 nm.

As mentioned earlier, the relatively inefficient step for this reaction system was the water reduction process on Pt/$BaZrO_3$−$BaTaO_2N$ catalysts. Therefore, the appreciable enhancement of gas evolution rates was due to the promotion of H_2 evolution on Pt/$BaZrO_3$−$BaTaO_2N$ catalysts by the addition of NaI. However, excess NaI addition had a negative effect on activity, along with a pronounced deviation in the H_2/O_2 ratio. Previous studies demonstrated that the competitive oxidation of I^- (backward reaction of eq 4) with water oxidation (eq 5) occurs on PtO_x/WO_3 when the concentration of I^- becomes high, thereby decreasing the rate of O_2 evolution.[7d,10b] As a result, the water-splitting rate gradually decreased with increasing NaI concentration above the 1−2 mM range.

It has also been reported that the pH of the reactant solution affects the overall efficiency of Z-scheme water splitting in the presence of an IO_3^-/I^- shuttle redox mediator, as does the concentration of NaI.[7d,10b] Because WO_3 is not suitable for pH-dependent experiments due to the inherent instability in basic solution,[7d] TiO_2 rutile, which has excellent chemical stability in both acidic and basic solution, was employed alternatively as an O_2 evolution photocatalyst. Supporting Information, Figure S5 shows the water splitting activities recorded using a mixture of Pt/$BaZrO_3$−$BaTaO_2N$ and TiO_2 rutile from aqueous NaI solution (1.0 mM) at various pH conditions. The activity was enhanced as the pH increased from 4.0 to 6.3, beyond which it began to drop gradually. The highest activity was obtained at pH 6.3 (without control), different from that recorded in a similar two-step water splitting system consisting of Pt/TiO_2 anatase and TiO_2 rutile. Abe et al. have reported that Z-scheme water splitting is achievable using a mixture of Pt/TiO_2 anatase and TiO_2 rutile in the presence of an IO_3^-/I^- shuttle redox mediator.[7a,d] In this system, a basic reaction condition (pH 11) was the most suitable because the oxidation of I^- into IO_3^- by Pt/TiO_2 anatase occurs efficiently. As the pH decreased, in contrast, the oxidation product tended to be I_3^- (see below, eq 10), which cannot work as an efficient electron acceptor for water oxidation over TiO_2 rutile.

$$3I^- + 2h^+ \rightarrow I_3^- \quad (\text{photooxidation of } I^- \text{ into } I_3^-) \qquad (10)$$

An activity drop observed in the present study from 6.3 to 4.0 would thus be due to more accumulation of I_3^-, as supported by the fact that the H_2/O_2 ratio in pH 4.0 was larger than that in pH 6.3 and that the color of the supernatant solution after reaction was pale brown, indicative of the production of I_3^-. I_3^- ions are also converted into I^- and IO_3^- via the following disproportional reaction:[25]

$$3I_3^- + 3H_2O \rightarrow 8I^- + IO_3^- + 6H^+ \qquad (11)$$

This reaction proceeds more smoothly in basic reaction condition than in acidic condition. As a result, the H_2/O_2 ratio in the reaction products would become larger than stoichiometric, even at the optimal NaI concentration. A drop in activity was also observed when the reaction pH for the Pt/$BaZrO_3$−$BaTaO_2N$ + PtO_x/WO_3 system was increased from 6.3 to 7.1 (data not shown). Thus, this characteristic pH dependent activity is ascribed to Pt/$BaZrO_3$−$BaTaO_2N$. Anyway, it appears that choosing nearly neutral pH is favorable for enhancing the activity of Pt/$BaZrO_3$−$BaTaO_2N$ as a H_2 evolution photocatalyst in Z-scheme water splitting.

3.6. Application of $BaZrO_3$−$BaTaO_2N$ as an O_2 Evolution Photocatalyst. Because $BaZrO_3$−$BaTaO_2N$ modified with colloidal IrO_2 as an O_2 evolution cocatalyst is capable of photocatalytically oxidizing water to produce O_2 in the presence of Ag^+ as an electron acceptor,[18] it is expected that water oxidation using this material is achievable even in a nonsacrificial manner, namely, using either IO_3^- or Fe^{3+} as a reversible electron acceptor. Thus, we examined water oxidation activities of $BaZrO_3$−$BaTaO_2N$ modified with various cocatalysts in aqueous $NaIO_3$ solution, and the results are listed in Table 3. $BaZrO_3$−$BaTaO_2N$ was inactive for water oxidation from aqueous $NaIO_3$ solution even under UV and visible irradiation (350 < λ < 800 nm), regardless of IrO_2 loading (entries 1 and 2, Table 3). Modification of $BaZrO_3$−$BaTaO_2N$ with Ru, Pt, or Ir species, which were reported to work as a reduction site for IO_3^-,[12b,15,17] did not yield O_2 production (entries 3−5). Interestingly, however, combining an IrO_2 water oxidation cocatalyst and Ru resulted in observable O_2 evolution (entry 6), while neither Pt nor Ir worked even in combination with IrO_2 (entries 7 and 8). Here, the loading amount of IrO_2 was 1.5 wt %, as has been optimized in the previous study.[18a] XPS analysis for $BaZrO_3$−$BaTaO_2N$ modified with Ru and IrO_2 showed that the valence state of the Ru species in this sample is close to Ru(IV) oxide (Supporting Information, Figure S6). Hence the Ru species loaded on $BaZrO_3$−$BaTaO_2N$ will be referred to as RuO_2 hereafter. TEM images showed that the size of the loaded RuO_2 was ~2 nm (Supporting Information, Figure S7). Our previous study has revealed that RuO_2 on TaON works as a bifunctional cocatalyst for TaON to promote the reduction of IO_3^- and the oxidation of water in a two-step water splitting system in the presence of an IO_3^-/I^- redox mediator.[12b] Thus, it is considered that in the present case, RuO_2 on $BaZrO_3$−$BaTaO_2N$ also undertakes the same job, but is likely to promote the reduction of IO_3^- rather than water oxidation, when combined with a colloidal IrO_2 cocatalyst that is known as being one of the most efficient water oxidation catalysts. Presumably, the oxidation of I^- would still be dominant on RuO_2/$BaZrO_3$−$BaTaO_2N$ judging from the inactivity of this sample (entry 3). Thus, it is most likely that IrO_2 loading needs to be done to improve the selectivity of the photogenerated holes to water oxidation. When the reaction was carried out in the presence of both IO_3^- and I^-, the rate of O_2 evolution decreased (entry 9). It indicates that the undesirable oxidation of I^- still occurs even after comodification with IrO_2.

While $BaZrO_3$−$BaTaO_2N$ modified with RuO_2 and IrO_2 was active for nonsacrificial water oxidation using IO_3^- as an electron acceptor, Z-scheme water splitting by combining either

Table 3. O_2 Evolution Activities of Modified $BaZrO_3$−$BaTaO_2N$ Photocatalysts from Aqueous $NaIO_3$ Solution[a]

entry	cocatalyst	reactant solution	amount of evolved O_2 for 10 h/μmol
1	none	$NaIO_3$ 10 mM	0
2	1.5 wt % IrO_2	$NaIO_3$ 10 mM	0
3	0.5 wt % Ru	$NaIO_3$ 10 mM	0
4	0.5 wt % Pt	$NaIO_3$ 10 mM	0
5	0.5 wt % Ir	$NaIO_3$ 10 mM	0
6	1.5 wt % IrO_2 + 0.5 wt % Ru	$NaIO_3$ 10 mM	3.2
7	1.5 wt % IrO_2 + 0.5 wt % Pt	$NaIO_3$ 10 mM	0
8	1.5 wt % IrO_2 + 0.5 wt % Ir	$NaIO_3$ 10 mM	0
9	1.5 wt % IrO_2 + 0.5 wt % Ru	$NaIO_3$ 10 mM + NaI 1.0 mM	1.4

[a] Reaction conditions: catalyst, 50 mg; aqueous solution, 100 mL; light source, xenon lamp (300 W) fitted with a cold mirror (CM-1); reaction vessel, Pyrex top-irradiation type; irradiation wavelength, 350 < λ < 800 nm.

Pt/TiO_2 or Pt/ZrO_2/TaON, both of which are effective H_2 evolution photocatalysts in an IO_3^-/I^- redox system,[7a,d,13a,b] could not be achieved; only H_2 was produced moderately under UV and visible irradiation.[26] Taking Pt/ZrO_2/TaON for example, stoichiometric H_2 and O_2 evolution is achieved when PtO_x/WO_3 is used as an O_2 evolution photocatalyst in a similar manner.[13a,b] Therefore, the inactivity of the $IrO_2/RuO_2/BaZrO_3-BaTaO_2N$-based system is ascribed to the low performance of the $IrO_2/RuO_2/BaZrO_3-BaTaO_2N$ component. Photoelectrochemical measurements revealed that the valence and conduction band-edge positions of $BaZrO_3-BaTaO_2N$ straddle the water splitting potential, but the valence band maximum of $BaZrO_3-BaTaO_2N$ is located at a potential close to the water oxidation potential.[18b] This might be one plausible explanation why $BaZrO_3-BaTaO_2N$ exhibits low activity for water oxidation.

3.7. Solar-Driven Z-scheme Water Splitting Using $BaZrO_3-BaTaO_2N$. On the basis of the results discussed above, it is concluded that $BaZrO_3-BaTaO_2N$ is more suitable as a H_2 evolution photocatalyst than for O_2 evolution at least in the present stage. The as-optimized Pt/$BaZrO_3-BaTaO_2N$ for H_2 evolution in the presence of an IO_3^-/I^- redox couple was then examined under simulated sunlight in combination with PtO_x/WO_3 and TiO_2 rutile as O_2 evolution photocatalysts. Solar energy conversion efficiency is the most reliable measure of a given photoactive system, as it can be compared to any of solar-driven energy transducers.

Figure 6 shows time courses of solar-driven Z-scheme water splitting. Both systems produced H_2 and O_2 stoichiometrically upon simulated sunlight, giving solar energy conversion efficiencies of 0.0067% for the Pt/$BaZrO_3-BaTaO_2N$ + Pt/WO_3 system and 0.014% for the Pt/$BaZrO_3-BaTaO_2N$ + TiO_2 rutile system, respectively. Thus, solar energy conversion using a $BaZrO_3-BaTaO_2N$ photocatalyst through Z-scheme water splitting was achieved.

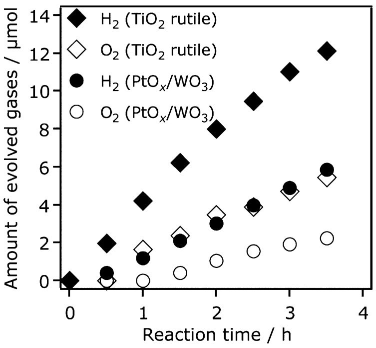

Figure 6. Time courses of solar-driven H_2 and O_2 evolution over a mixture of 0.3 wt % Pt/$BaZrO_3-BaTaO_2N$ and either PtO_x/WO_3 and TiO_2 rutile. Reaction conditions: catalyst, 100 mg of PtO_x/WO_3 (or TiO_2 rutile) and 50 mg of Pt/$BaZrO_3-BaTaO_2N$; aqueous NaI solution, 100 mL (1.0 mM); light source, solar simulator; reaction vessel, Pyrex top-irradiation type.

It should be noted that H_2-O_2 recombination (eq 12 below), which is thermodynamically favorable, takes place on Pt/$BaZrO_3-BaTaO_2N$ during the reaction.

$$2H_2 + O_2 \rightarrow 2H_2O \tag{12}$$

This was confirmed by testing the water formation reaction from a mixture of H_2 and O_2 in the dark using Pt/$BaZrO_3-BaTaO_2N$. As shown in Supporting Information, Figure S8, the amounts of H_2 and O_2 in a closed-gas circulation system containing Pt/$BaZrO_3-BaTaO_2N$ in aqueous NaI solution both decreased with time while maintaining the stoichiometric ratio. In contrast, no H_2-O_2 consumption was observed on PtO_x/WO_3 and TiO_2 rutile. These results indicate that water formation occurs on a Pt/$BaZrO_3-BaTaO_2N$; more specifically on metallic Pt nanoparticles. For PtO_x/WO_3, Pt species in this material consist of Pt(II) oxide as the majority species, with a small contribution of metallic Pt species.[10b,17] Thus, the water formation on PtO_x/WO_3 would be very slow. It is thus clear that, during photocatalytic water splitting, this undesirable reaction occurs, thereby reducing the detected rates of H_2 and O_2 evolution. Suppressing the backward reaction is another important task toward efficient Z-scheme water splitting.

4. CONCLUSIONS

We attempted to construct photocatalytic water splitting systems driven by two-step photoexcitation of two different semiconductor photocatalysts using a modified $BaZrO_3-BaTaO_2N$ solid solution with a band gap of 1.8 eV. Despite the low band gap energy to drive water reduction and oxidation, the solid solutions modified with suitable cocatalysts were shown to produce H_2 or O_2 in the presence of reversible redox couples (viz. IO_3^-/I^- and Fe^{3+}/Fe^{2+}), achieving non-sacrificial water reduction or oxidation. Solar-driven Z-scheme water splitting was demonstrated using $BaZrO_3-BaTaO_2N$ modified with Pt nanoparticles as water reduction promoters, in combination with either PtO_x/WO_3 or TiO_2 rutile as an O_2 evolution photocatalyst in the presence of an IO_3^-/I^- shuttle redox mediator. Although Z-scheme water splitting using only $BaZrO_3-BaTaO_2N$ has not been achieved so far due primarily to the insufficient quality of the material, the results of the present study clearly demonstrate the possibility of a non-sacrificial water splitting system consisting only of photocatalysts with band gaps smaller than 2 eV after further refinement of catalyst preparation to suppress the undesirable backward reactions.

■ ASSOCIATED CONTENT

Ⓢ Supporting Information

Characterization and reaction data. This material is available free of charge via the Internet at http://pubs.acs.org.

■ AUTHOR INFORMATION

Corresponding Author

*Phone: +81-3-5734-2239 (K.M.), +81-3-5841-8838 (K.D.). Fax: +81-3-5734-2284 (K.M.), +81-3-5841-1652 (K.D.). E-mail: maedak@chem.titech.ac.jp (K.M.), domen@chemsys.t.u-tokyo.ac.jp (K.D.).

Notes

The authors declare no competing financial interest.

■ ACKNOWLEDGMENTS

This work was supported by the PRESTO/JST program “Chemical Conversion of Light Energy”. The authors would also like to acknowledge the Grant-in-Aid for Specially Promoted Research (No. 23000009) of the Ministry of Education, Culture, Sports, Science, and Technology (MEXT) of Japan, and Advanced Low Carbon Technology Research and Development Program (ALCA) of the Japan Science and Technology Agency (JST). One of the authors

(K.M.) thanks the Nippon Sheet Glass Foundation for Materials Science and Engineering for funding support.

REFERENCES

(1) Maeda, K.; Domen, K. *J. Phys. Chem. Lett.* **2010**, *1*, 2655.

(2) (a) Kudo, A.; Miseki, Y. *Chem. Soc. Rev.* **2009**, *38*, 253. (b) Abe, R. *J. Photochem. Photobiol., C* **2010**, *11*, 179. (c) Maeda, K. *J. Photochem. Photobiol., C* **2011**, *12*, 237. (d) Wang, Y.; Wang, X.; Antonietti, M. *Angew. Chem., Int. Ed.* **2012**, *51*, 68.

(3) Bard, A. J. *J. Photochem.* **1979**, *10*, 59.

(4) Tennakone, K.; Wickramanayake, S. *J. Chem. Soc., Faraday Trans. 2* **1986**, *82*, 1475.

(5) (a) Sayama, K.; Yoshida, R.; Kusama, H.; Okabe, K.; Abe, Y.; Arakawa, H. *Chem. Phys. Lett.* **1997**, *277*, 387. (b) Bamwenda, G. R.; Sayama, K.; Arakawa, H. *J. Photochem. Photobiol., A* **1999**, *122*, 175.

(6) (a) Fujihara, K.; Ohno, T.; Matsumura, M. *J. Chem. Soc., Faraday Trans.* **1998**, *94*, 3705. (b) Ohno, T.; Haga, D.; Fujihara, K.; Kaizaki, K.; Matsumura, M. *J. Phys. Chem. B* **1997**, *101*, 6415.

(7) (a) Abe, R.; Sayama, K.; Domen, K.; Arakawa, H. *Chem. Phys. Lett.* **2001**, *344*, 339. (b) Sayama, K.; Mukasa, K.; Abe, R.; Abe, Y.; Arakawa, H. *Chem. Commun.* **2001**, 2416. (c) Sayama, K.; Mukasa, K.; Abe, R.; Abe, Y.; Arakawa, H. *J. Photochem. Photobiol., A* **2002**, *148*, 71. (d) Abe, R.; Sayama, K.; Sugihara, H. *J. Phys. Chem. B* **2005**, *109*, 16052.

(8) Sayama, K.; Abe, R.; Arakawa, H.; Sugihara, H. *Catal. Commun.* **2006**, *7*, 96.

(9) (a) Kato, H.; Hori, M.; Konta, R.; Shimodaira, Y.; Kudo, A. *Chem. Lett.* **2004**, *33*, 1348. (b) Kato, H.; Sasaki, Y.; Iwase, A.; Kudo, A. *Bull. Chem. Soc. Jpn.* **2007**, *80*, 2457. (c) Sasaki, Y.; Iwase, A.; Kato, H.; Kudo, A. *J. Catal.* **2008**, *259*, 133. (d) Sasaki, Y.; Nemoto, H.; Saito, K.; Kudo, A. *J. Phys. Chem. C* **2009**, *113*, 17536.

(10) (a) Abe, R.; Takata, T.; Sugihara, H.; Domen, K. *Chem. Commun.* **2005**, 3829. (b) Abe, R.; Higashi, M.; Domen, K. *ChemSusChem* **2011**, *4*, 228.

(11) (a) Higashi, M.; Abe, R.; Teramura, K.; Takata, T.; Ohtani, B.; Domen, K. *Chem. Phys. Lett.* **2008**, *452*, 120. (b) Higashi, M.; Abe, R.; Takata, T.; Domen, K. *Chem. Mater.* **2009**, *21*, 1543.

(12) (a) Higashi, M.; Abe, R.; Ishikawa, A.; Takata, T.; Ohtani, B.; Domen, K. *Chem. Lett.* **2008**, *37*, 138. (b) Maeda, K.; Abe, R.; Domen, K. *J. Phys. Chem. C* **2011**, *115*, 3057.

(13) (a) Maeda, K.; Terashima, H.; Kase, K.; Higashi, M.; Tabata, M.; Domen, K. *Bull. Chem. Soc. Jpn.* **2008**, *81*, 927. (b) Maeda, K.; Higashi, M.; Lu, D.; Abe, R.; Domen, K. *J. Am. Chem. Soc.* **2010**, *132*, 5858. (c) Ma, S. S. K.; Maeda, K.; Domen, K. *Catal. Sci. Technol.* **2012**, *2*, 818.

(14) Abe, R.; Shinmei, K.; Hara, K.; Ohtani, B. *Chem. Commun.* **2009**, 3577.

(15) Tabata, M.; Maeda, K.; Higashi, M.; Lu, D.; Takata, T.; Abe, R.; Domen, K. *Langmuir* **2010**, *26*, 9161.

(16) Matoba, T.; Maeda, K.; Domen, K. *Chem.—Eur. J.* **2011**, *17*, 14731.

(17) Ma, S. S. K.; Maeda, K.; Abe, R.; Domen, K. *Energy Environ. Sci.* **2012**, *5*, 8390.

(18) (a) Maeda, K.; Domen, K. *Angew. Chem., Int. Ed.* **2012**, *51*, 9865. (b) Maeda, K.; Domen, K. *J. Catal.* 2013, in press. DOI: 10.1016/j.jcat.2012.12.003.

(19) Iwase, A.; Kato, H.; Kudo, A. *J. Sol. Energy Eng.* **2010**, *132*, 021106.

(20) Harriman, A.; Pickering, I. J.; Thomas, J. M.; Christensen, P. A. *J. Chem. Soc., Faraday Trans. 1* **1988**, *84*, 2795.

(21) Maeda, K.; Higashi, M.; Siritanaratkul, B.; Abe, R.; Domen, K. *J. Am. Chem. Soc.* **2011**, *133*, 12334.

(22) Teratani, S.; Nakamichi, J.; Taya, K.; Tanaka, K. *Bull. Chem. Soc. Jpn.* **1982**, *55*, 1688.

(23) (a) Iwase, A.; Kato, H.; Kudo, A. *Catal. Lett.* **2006**, *108*, 7. (b) Gärtner, F.; Losse, S.; Boddien, A.; Pohl, M.-M.; Denurra, S.; Junge, H.; Beller, M. *ChemSusChem* **2012**, *5*, 530.

(24) Kim, K. S.; Winograd, N.; Davis, R. E. *J. Am. Chem. Soc.* **1971**, *93*, 6296.

(25) Dushman, P. *J. Phys. Chem.* **1904**, *8*, 481.

(26) Pt/TiO_2 was prepared by an in-situ photodeposition method in a similar manner previously reported (Kraeutler, B.; Bard, A. J. *J. Am. Chem. Soc.* **1978**, *100*, 4317.). A TiO_2 powder (JRC-TIO-4), one of the most active TiO_2 photocatalysts for H_2 evolution (Prieto-Mahaney, O. O.; Murakami, N.; Abe, R.; Ohtani, B. *Chem. Lett.* **2009**, *38*, 238), was supplied by The Catalysis Society of Japan.